TECHNICAL NOTE

D-742

HOVERING CHARACTERISTICS OF A ROTOR HAVING AN AIRFOIL SECTION DESIGNED FOR FLYING-CRANE TYPE OF HELICOPTER

By James P. Shivers

Langley Research Center
Langley Field, Va.

NATIONAL AERONAUTICS AND SPACE ADMINISTRATION

WASHINGTON April 1961

NATIONAL AERONAUTICS AND SPACE ADMINIS

TECHNICAL NOTE D-742

HOVERING CHARACTERISTICS OF A ROTOR HAVING AN AIRFOIL SECTION DESIGNED FOR FLYING-CRANE TYPE OF HELICOPTER

By James P. Shivers

SUMMARY

Results of an investigation, conducted on the Langley helicopter test tower, of a rotor having an NACA 63_2A015 airfoil thickness distribution in combination with an NACA 230 mean line are presented. Comparison with a previously reported test of a symmetrical rotor blade having similar thickness distribution indicates that the present rotor efficiency was substantially improved over a wide range of tip Mach numbers. The maximum mean lift coefficient was essentially unchanged from that obtained with uncambered blades. Some data showing the effect of a distributed type of leading-edge roughness are also included.

INTRODUCTION

Rotor hovering efficiency is very important in the design of a flying-crane type of helicopter. A given percentage increase in the rotor thrust at constant power generally represents a percentage increase in payload several times as large. The effects of rotor blade geometry and tip speed on the hovering efficiency are fairly well understood and predictable (see ref. 1), at least for values representative of current design practice. Once the best compromise of geometry and tip speed are selected, further gains in hovering efficiency can be made by reduction of the profile power of the airfoil section. In such case the practical problem is to design an airfoil section which has inherently low drag at the operating values of the lift coefficient. In reference 2 the use of camber to accomplish this low drag is indicated, and this paper reports one attempt to develop such an airfoil with the special requirements of helicopters considered.

Factors influencing the choice of the NACA 63_2A015 airfoil thickness distribution in combination with an NACA 230 mean line were the

efficient performance over wide ranges of mean lift coefficients and blade tip Mach numbers shown by the NACA 63_2-015 airfoil section (see ref. 3) and the improved airfoil section efficiency obtainable without significant quarter-chord pitching moments by the use of forward camber. The NACA 63_2A015 thickness distribution was used in lieu of the NACA 63_2-015 to avoid structural problems associated with a cusped trailing edge. The two airfoils are essentially similar from the aerodynamic standpoint. (See refs. 4 and 5.)

The rotor blades were tested on the Langley helicopter test tower to determine the force data on smooth blades over a range of tip Mach numbers from 0.35 to 0.67 with corresponding blade tip Reynolds numbers from 2.25×10^6 to 4.36×10^6. In addition, data were obtained for two different conditions of a distributed type of leading-edge roughness to determine their effect on the rotor performance.

SYMBOLS

b number of blades

c blade chord at radius r, ft

$c_{d,o}$ airfoil section profile-drag coefficient

c_e equivalent blade chord, $\dfrac{\int_0^R cr^2 dr}{\int_0^R r^2 dr}$ (on thrust basis), ft

c_l airfoil section lift coefficient

$\bar{c}_l$ rotor blade mean lift coefficient, $6C_T/\sigma$

C_m rotor blade pitching-moment coefficient, $\dfrac{M_Y}{\frac{R\rho}{2}(\Omega R)^2 c_e^2}$

C_Q rotor torque coefficient, $\dfrac{Q}{\pi R^2 \rho (\Omega R)^2 R}$

$C_{Q,o}$ rotor profile-drag torque coefficient, $\frac{Q_o}{\pi R^2 \rho (\Omega R)^2 R}$

C_T rotor thrust coefficient, $\frac{T}{\pi R^2 \rho (\Omega R)^2}$

M_t rotor blade tip Mach number

M_Y rotor blade pitching moment, lb-ft

N_{Re} Reynolds number at blade tip, $\frac{\rho \Omega R c_t}{\mu}$

Q rotor torque, lb-ft

Q_o rotor profile-drag torque, lb-ft

r radial distance to a blade element, ft

R rotor blade radius, ft

T rotor thrust, lb

α_r blade section angle of attack, deg or radians, as specified

θ blade section pitch angle measured from line of zero lift at 0.75R or tip, as specified, deg

μ coefficient of viscosity, slugs/ft-sec

ρ mass density of air, slugs/cu ft

σ rotor solidity, $bc_e/\pi R$

Ω rotor angular velocity, radians/sec

Subscripts:

max maximum

t at blade tip

The figure of merit is equal to $0.707 C_T^{3/2} / C_Q$.

APPARATUS AND TESTS

Rotor Blades

The rotor used for this investigation was a fully articulated, two-blade rotor with flapping hinges located at the center of rotation and drag hinges located at the 5.35-percent spanwise station.

A sketch of the rotor blade with pertinent dimensions is shown in figure 1. The rotor solidity was 0.03, the radius was 18.71 feet, the pitch axis was located at 0.23c, and the twist distribution was as indicated in figure 1. The outer approximately 60 percent of the rotor blade was contoured to an NACA 63_2A015 airfoil thickness distribution in combination with an NACA 230 mean line (designated in fig. 1 as NACA 63_2A015 (230 mean line) airfoil section). The stations and ordinates for the airfoil section are given in table I. The airfoil surface was smooth and fair over the entire blade.

In order to determine the extent to which the rotor performance would be affected by a distributed type of leading-edge roughness (refs. 6 and 7), some tests were made with roughness applied to both upper and lower surfaces for a surface distance of 0.08c measured rearward from the leading edge. Tests were made first with a coat of brush-applied shellac, for which spanwise brush marks were measured to be from 0.002 to 0.004 inch in height. The second condition consisted of a fresh coating of shellac to which No. 120 carborundum particles (nominal size 0.0049 inch) were applied. The particles covered 5 to 10 percent of the area, and the total roughness height varied from 0.006 to 0.009 inch (0.007 inch average).

Test Methods and Accuracy

The test procedure was the same as that of references 3, and 8 to 10 in that the blades were rotated in hovering for a series of rotor tip speeds at various blade pitch settings within allowable blade stress levels. In these tests, however, the rotor tip was photographed at each pitch angle and tip Mach number in order to determine the amount of dynamic twist. A sample photograph is shown in figure 2. The dynamic twist at the blade tip (fig. 3) was determined as the difference between the preselected tip pitch angle, calculated from the measured blade root pitch angle plus known geometric twist, and the photographed tip pitch angle. With this technique significant amounts of dynamic twist were measured $\left(\text{up to } 5^\circ \text{ or } 5\frac{1}{2}^\circ \text{ nosedown}\right)$ for high tip Mach numbers and low tip pitch angles (0° to 3°). The dynamic twist becomes less negative for

tip pitch angles from 3° to 10°, and above 10° the nosedown twist increases slightly as the pitch is increased to the maximum tested. The accuracy to which the photographed tip angle could be read is approximately 12 minutes.

In order to provide a basis for estimating the distribution of dynamic twist along the rotor blade, the spanwise blade twisting deformations were determined with a moment applied at the blade tip. For the present rotor blade, the dynamic twist at 0.75R was determined as 49 percent of that at the blade tip. (See fig. 1.) The spanwise distribution of the dynamic twist measured from the photographs made during the tests was assumed to be the same as that for the static distribution.

The estimated accuracies of the plotted results of the basic quantities measured during the tests are believed to be within ±3 percent.

METHOD OF ANALYSIS

A good indication of the presence of rotor blade stalling or compressibility drag rise is afforded by inspection of the profile-drag torque coefficient. For previous investigations (refs. 3, and 8 to 10) calculations based on the conventional airfoil drag polar $\left(c_{d,o} = 0.0087 - 0.0216\alpha_r + 0.400\alpha_r^2\right)$ have closely approximated the measured performance at low tip speeds. The conventional polar, however, does not adequately represent the drag of the present blades which indicate greater efficiency over a wide range of thrust coefficients. For this reason the profile-drag torque coefficients deduced from the tests have been referenced to the values of $C_{Q,o}$ obtained from the $M_t = 0.35$ curve in figure 4. The extrapolated portion of the $M_t = 0.35$ reference curve was determined by sketching a curve parallel to the calculated incompressible no-stall curve. The point at which the $M_t = 0.35$ curve deviates from the extrapolated curve indicates the onset of drag divergence for the low-speed curve.

RESULTS AND DISCUSSION

Results Obtained for Smooth Rotor Blades

The rotor performance and efficiency characteristics, measured over a range of tip Mach numbers and a range of pitch angles, are presented in figures 4 to 6. In figure 4 the rotor performance for the smooth blades is presented along with a calculated incompressible no-stall curve

and a calculated induced-torque-coefficient curve. The extrapolated $M_t = 0.35$ curve is used for the incompressible no-stall reference curve for determination of the ratios of the profile-drag coefficients presented in figures 7 and 8. Figure 4 shows that a maximum mean lift coefficient $\bar{c}_{l,max}$ of 1.16 was measured for the test rotor. This value was essentially the same as that obtained on a rotor having a similar airfoil thickness distribution (see ref. 3), but no camber. The adverse effect of Mach number on the $\bar{c}_{l,max}$ in the test operating range (see ref. 11) together with the likelihood of some inboard stalling (as experienced in ref. 12) constitute possible explanations. Drag divergence was indicated at zero thrust at a tip Mach number value of 0.67. This low value for drag divergence at this tip Mach number (see ref. 3) is believed to be caused by the large amount of dynamic twist.

Figure 5 shows the variation of rotor thrust coefficient with blade section pitch angle for various tip Mach numbers. The calculated incompressible curve was computed by use of a section-lift-curve slope of 5.73. In the lower thrust-coefficient range the experimental curve slopes fall below that of the calculated curve which indicates that the slope of the lift curve is less than 5.73. As tip Mach number is increased with increased pitch angle the slopes of the experimental curves reach values above that of the calculated curve. The curves show a characteristic shape similar to those of the previous investigations of references 3 and 8 to 10.

The effect of tip Mach number on rotor blade efficiency, expressed as a figure of merit, is shown in figure 6. At tip Mach numbers of 0.54 and below the figure shows figures of merit between 0.75 and 0.80 over a wide range of mean lift coefficients ($\bar{c}_l = 0.50$ to 0.93). At the higher tip Mach numbers of 0.63 and 0.67 the compressibility losses reduce the maximum figure of merit to 0.715 and 0.705, respectively.

Effects of Tip Mach Number on Ratios of Profile-Drag Torque Coefficients

The ratios of the profile-drag torque coefficients are presented as functions of rotor blade tip angle of attack and rotor blade mean lift coefficient in figures 7 and 8, respectively. The present calculations for tip angle of attack are corrected for the measured dynamic twist whereas this measurement was not available for inclusion in the calculations of references 3 and 8 to 10. In the low and intermediate range of blade tip angle of attack (or rotor mean lift coefficient), the test rotor experienced much less favorable profile-drag divergence characteristics than did the uncambered rotor of reference 3. In

general, the shapes of the curves of figures 7 and 8, however, are quite similar to those of reference 3 in that they are characterized by a small initial rate of increase in the ratio of the profile-drag coefficients. A much more rapid rise in the profile power is indicated as the values of $\alpha_{r,t}$ or $\bar{c}_l$ are increased.

Rotor-Blade Pitching Moments

A comparison of the blade pitching-moment characteristics for representative tip Mach numbers of 0.35 to 0.67 as a function of rotor thrust coefficient for the rotor tested (smooth condition) is shown in figure 9. The pitching-moment data represent the measured rotor blade moments about the blade pitch axis (located at 0.23c) and include aerodynamic and blade mass forces. The resultant moment is shown to be small (that is, less than 70 foot-pounds) and positive over most of the thrust-coefficient range. In this respect, the presence or absence of abrupt changes in the pitching-moment coefficient is of more significance than the actual magnitude of the pitching moments. As the tip Mach number is increased in the low thrust-coefficient range, there is a progressive decrease in the pitching moments. This decrease in pitching moment is associated with the known rearward shift of the chordwise aerodynamic loading that occurs as the Mach number is increased.

Effect of Roughness

The effect of leading-edge roughness on rotor efficiency is shown in figure 10 where the rotor figure of merit is plotted as a function of tip Mach number for various values of mean lift coefficient.

The figure shows that the addition of shellac alone had an almost negligible effect on the rotor efficiency. This is not too surprising because the local velocities along the blade defined by the present test program are generally below those required for incipient transition to occur for the brush-mark heights previously quoted. (See refs. 8 and 9.) When the No. 120 carborundum particles were added to the leading edge, however, the efficiency decrease ranged from 22 percent to 15 percent at $\bar{c}_l = 0.3$ over the blade tip Mach number range and ranged from 12 percent to 9 percent at $\bar{c}_l = 0.7$.

Comparison of Cambered and Uncambered Blades

The Mach numbers for drag divergence of the cambered blade of this report with and without the effect of the dynamic twist are presented in figure 11 along with the results obtained for the rotor of reference 3.

The rotor of reference 3 was not corrected for dynamic twist and therefore cannot be compared to the rotor of the present investigation which takes into account the dynamic twist. The difference between the two uncorrected curves represents the effect of the camber and, quite probably, different amounts of dynamic twist.

Despite the probable difference in blade twist, a comparison of the effects of tip Mach number on rotor efficiency of cambered and uncambered blades at several values of mean lift coefficients is presented in figure 12. This figure shows that the cambered blades achieved substantial gains in efficiency over a wide range of Mach numbers. The solidity of the uncambered blades was 0.0374. For the blades of the present test, the solidity was 0.030. From a consideration of solidity only, the rotor of reference 3 should obtain approximately 1.5 percent higher maximum figures of merit because of its higher solidity; thus, the gains shown for the cambered blades would be increased if a theoretical allowance for solidity were made. Because blade surface conditions were generally comparable, the primary source of the improvement shown by the present blades is attributed to camber.

Since the cambered blades do show favorable gains in rotor efficiency for tip Mach number values of 0.54 and below, this fact would suggest a design choice of rotational tip speed below that of conventional helicopters. The choice of tip speed for conventional helicopters, however, has been influenced by the fact that at high forward speeds, high tip speeds offer numerous advantages. Because the load-lifter type of helicopter is mainly concerned with high lifting efficiency in hovering and is not expected to be capable of high forward speed, it would appear that an airfoil having the thickness distribution of an NACA 63_2A015 airfoil section in combination with an NACA 230 mean line would be well suited for the rotor of such a machine.

CONCLUSIONS

A full-scale rotor having blades with a special cambered airfoil section (NACA 63_2A015 airfoil thickness distribution in combination with an NACA 230 mean line) has been tested for static thrust. Examination of the data indicates the following conclusions:

1. A maximum rotor blade mean lift coefficient of 1.16 was obtained for the rotor with cambered blades. This value was essentially the same as that obtained on a rotor having a similar airfoil thickness distribution, but no camber.

2. The rotor had maximum figures of merit from 0.75 to 0.80 over a range of mean lift coefficients from 0.50 to 0.93 at tip Mach numbers of 0.54 and below.

3. When a distributed type of leading-edge roughness was added to the rotor blade, the efficiency decrease ranged from 22 percent to 15 percent at a rotor blade mean lift coefficient of 0.3 over the blade tip Mach number range. At a rotor blade mean lift coefficient of 0.7, the reduction in efficiency ranged from 12 percent to 9 percent.

4. The pitching moments were small and noseup occurred over most of the thrust-coefficient range. There were no abrupt changes in pitching moment over the thrust-coefficient range investigated.

5. By use of photographic techniques, significant amounts of dynamic twist were measured $\left(\text{up to } 5^\circ \text{ or } 5\frac{1}{2}^\circ \text{ nosedown}\right)$ at low tip pitch settings and high tip Mach numbers.

6. Favorable gains in rotor efficiency for tip Mach number values of 0.54 and below, achieved as a result of camber, would favor a design choice of tip Mach numbers below those of conventional helicopters. An airfoil having the thickness distribution of an NACA 63_2A015 airfoil section in combination with an NACA 230 mean line appears to be well suited for a load-lifter type of helicopter since this type of helicopter has less to gain from high tip speeds in the forward-flight regime.

Langley Research Center,
National Aeronautics and Space Administration,
Langley Field, Va., January 10, 1961.

REFERENCES

1. Gessow, Alfred, and Myers, Garry C., Jr.: Aerodynamics of the Helicopter. The Macmillan Co., c.1952.

2. Abbott, Ira H., Von Doenhoff, Albert E., and Stivers, Louis S., Jr.: Summary of Airfoil Data. NACA Rep. 824, 1945. (Formerly NACA WR L-560.)

3. Shivers, James P., and Carpenter, Paul J.: Experimental Investigation on the Langley Helicopter Test Tower of Compressibility Effects on a Rotor Having NACA 63_2-015 Airfoil Sections. NACA TN 3850, 1956.

4. Loftin, Laurence K., Jr.: Theoretical and Experimental Data for a Number of NACA 6A-Series Airfoil Sections. NACA Rep. 903, 1948. (Supersedes NACA TN 1368.)

5. Lindsey, W. F., and Humphreys, Milton D.: Tests of the NACA 64_1-012 and 64_1A012 Airfoils at High Subsonic Mach Numbers. NACA RM L8D23, 1948.

6. Braslow, Albert L., and Knox, Eugene C.: Simplified Method for Determination of Critical Height of Distributed Roughness Particles for Boundary-Layer Transition at Mach Numbers From 0 to 5. NACA TN 4363, 1958.

7. Von Doenhoff, Albert E., and Horton, Elmer A.: A Low-Speed Experimental Investigation of the Effect of a Sandpaper Type of Roughness on Boundary-Layer Transition. NACA Rep. 1349, 1958. (Supersedes NACA TN 3858.)

8. Powell, Robert D., Jr., and Carpenter, Paul J.: Low Tip Mach Number Stall Characteristics and High Tip Mach Number Compressibility Effects on a Helicopter Rotor Having an NACA 0009 Tip Airfoil Section. NACA TN 4355, 1958.

9. Carpenter, Paul J.: Lift and Profile-Drag Characteristics of an NACA 0012 Airfoil Section as Derived From Measured Helicopter-Rotor Hovering Performance. NACA TN 4357, 1958.

10. Powell, Robert D., Jr.: Compressibility Effects on a Hovering Helicopter Rotor Having an NACA 0018 Root Airfoil Tapering to an NACA 0012 Tip Airfoil. NACA RM L57F26, 1957.

11. Racisz, Stanley F.: Effects of Independent Variations of Mach Number and Reynolds Number on the Maximum Lift Coefficients of Four NACA 6-Series Airfoil Sections. NACA TN 2824, 1952.

12. Shivers, James P., and Carpenter, Paul J.: Effects of Compressibility on Rotor Hovering Performance and Synthesized Blade-Section Characteristics Derived From Measured Rotor Performance of Blades Having NACA 0015 Airfoil Tip Sections. NACA TN 4356, 1958.

TABLE I.- ORDINATES OF NACA 63_2A015 (230 MEAN LINE)

AIRFOIL SECTION

[Stations and ordinates given in percent of airfoil chord]

Upper surface		Lower surface	
Station	Ordinate	Station	Ordinate
0	0	0	0
.166	1.305	.834	-1.007
.358	1.614	1.142	-1.174
.776	2.139	1.724	-1.425
1.924	3.180	3.076	-1.848
4.416	4.726	5.584	-2.416
7.031	5.849	7.969	-2.865
9.692	6.689	10.308	-3.287
15.001	7.780	14.999	-4.104
20.146	8.384	19.854	-4.850
25.157	8.745	24.843	-5.433
30.163	8.928	29.837	-5.836
35.166	8.930	34.834	-6.058
40.164	8.758	39.836	-6.108
45.160	8.428	44.840	-5.998
50.151	7.960	49.849	-5.752
55.142	7.380	54.858	-5.390
60.129	6.702	59.871	-4.936
65.115	5.946	64.885	-4.398
70.099	5.129	69.901	-3.805
75.083	4.283	74.917	-3.177
80.066	3.432	79.934	-2.548
85.050	2.583	84.950	-1.919
90.033	1.733	89.967	-1.291
95.017	.882	94.983	-.662
100.001	.032	99.999	-.032

L.E. radius: 1.63
Slope of radius through L.E.: 0.3051

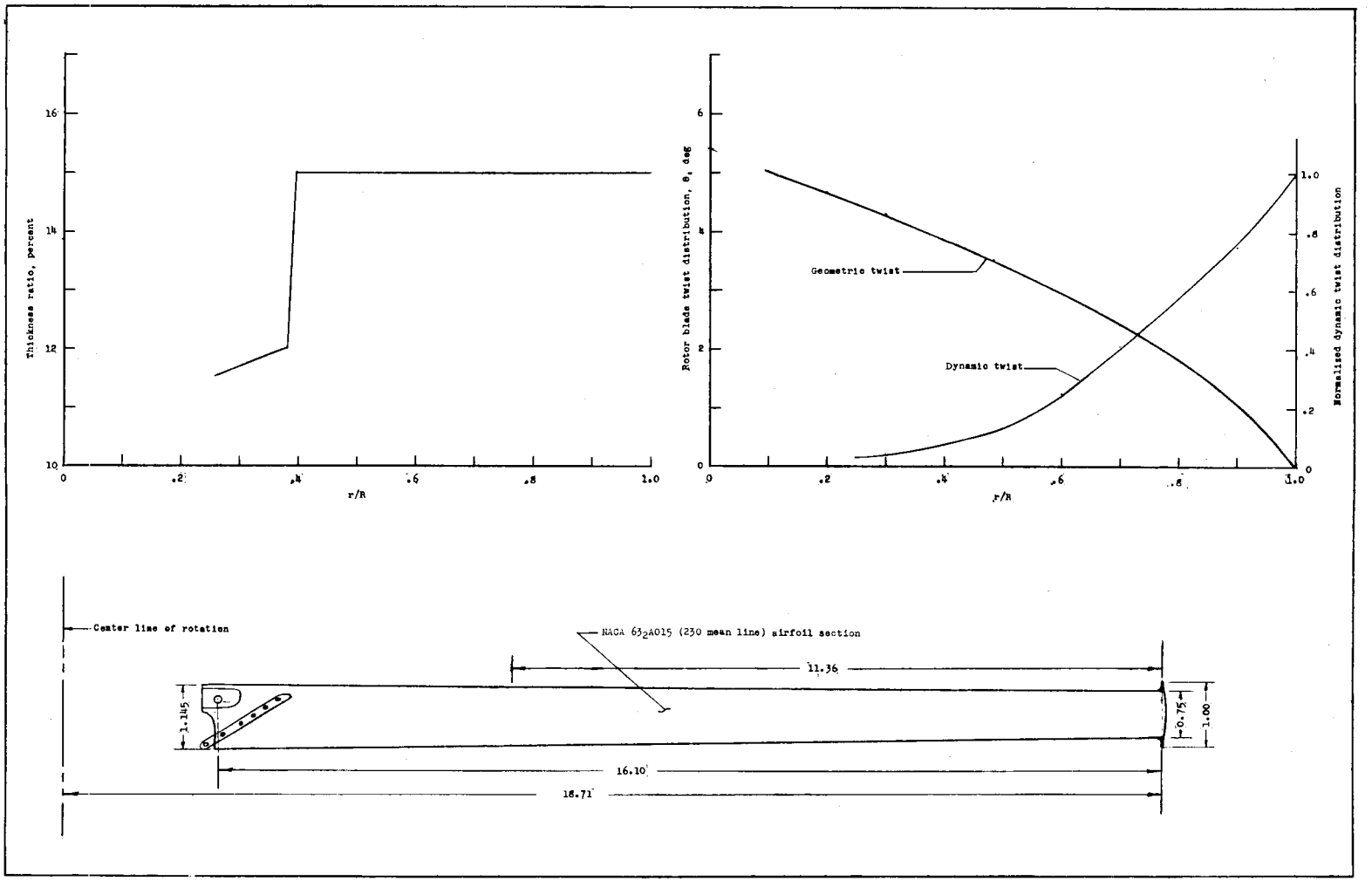

Figure 1.- Sketch of rotor blade having NACA 63_2A015 airfoil section with a 230 mean line over outer approximately 60 percent of blade radius. Equivalent blade chord = 0.885; σ = 0.030. All dimensions are in feet.

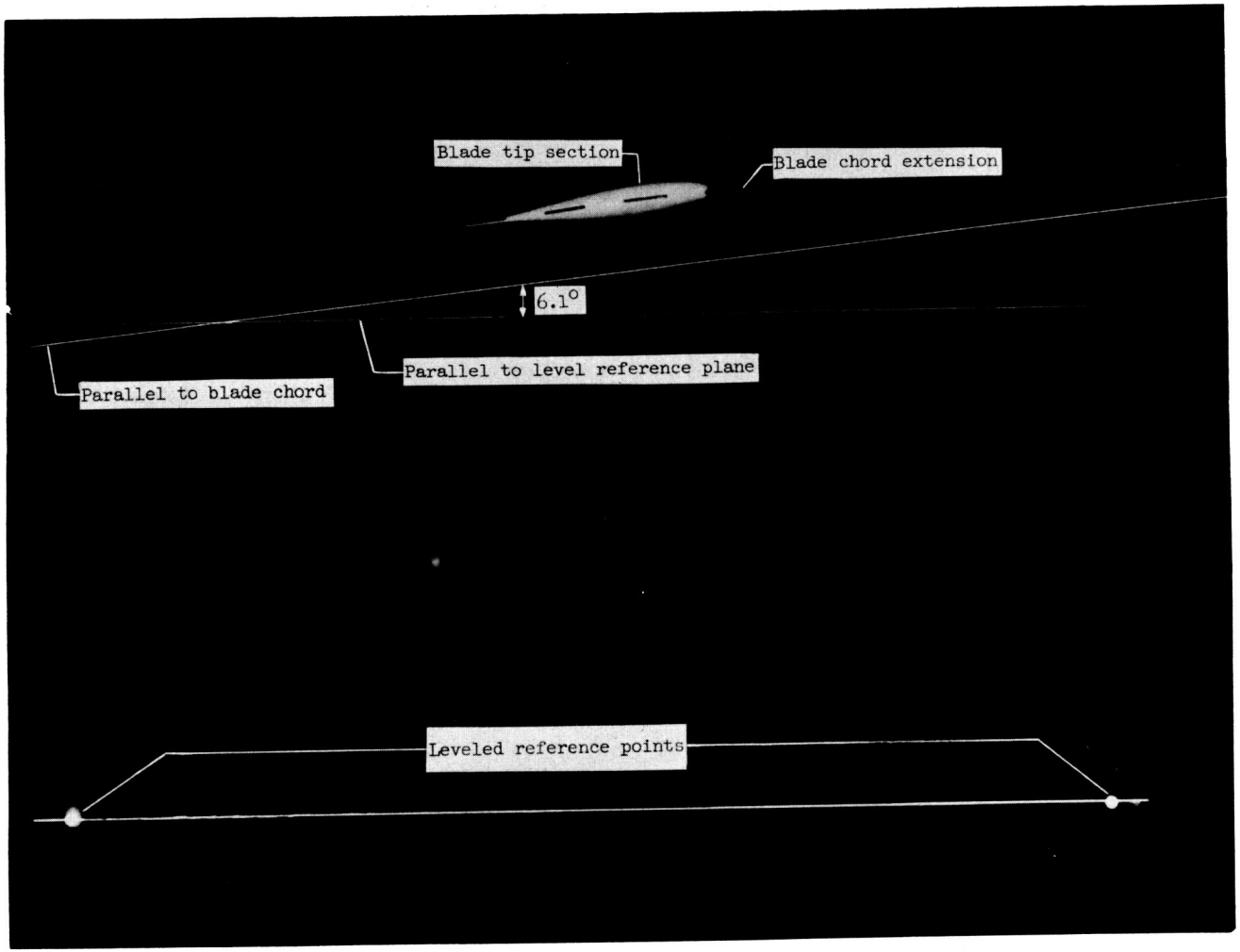

L-61-28

Figure 2.- Typical photograph of rotor blade tip. Tip speed 393 fps; $C_T = 0.003187$; $C_Q = 0.0001648$.

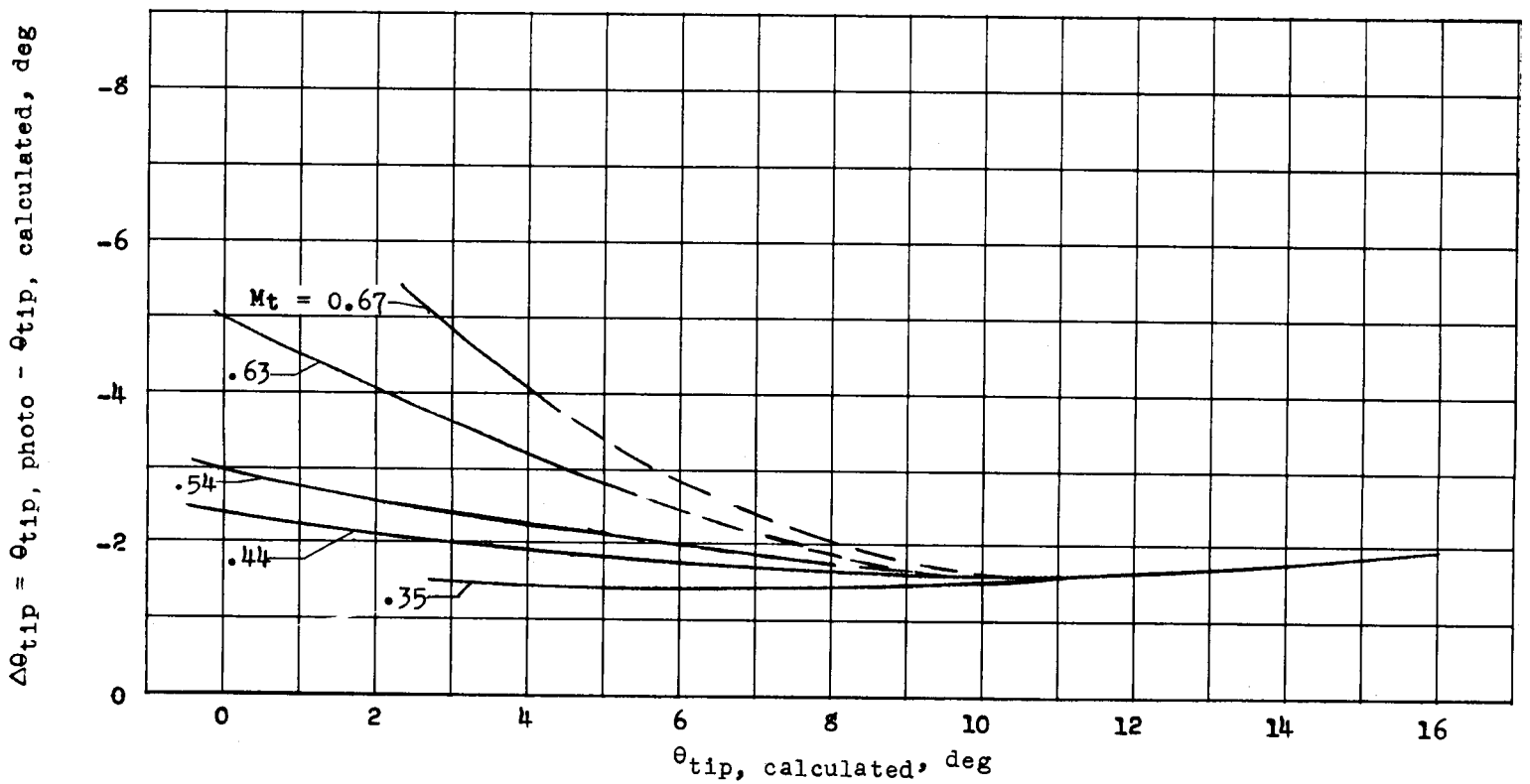

Figure 3.- Effect of tip Mach number on rotor blade dynamic twist.
$\theta_{tip,calculated} = \theta_{root,measured} + \theta_1$, where θ_1 = geometric twist of rotor blade.
The dashed portion of curves represents extrapolated data.

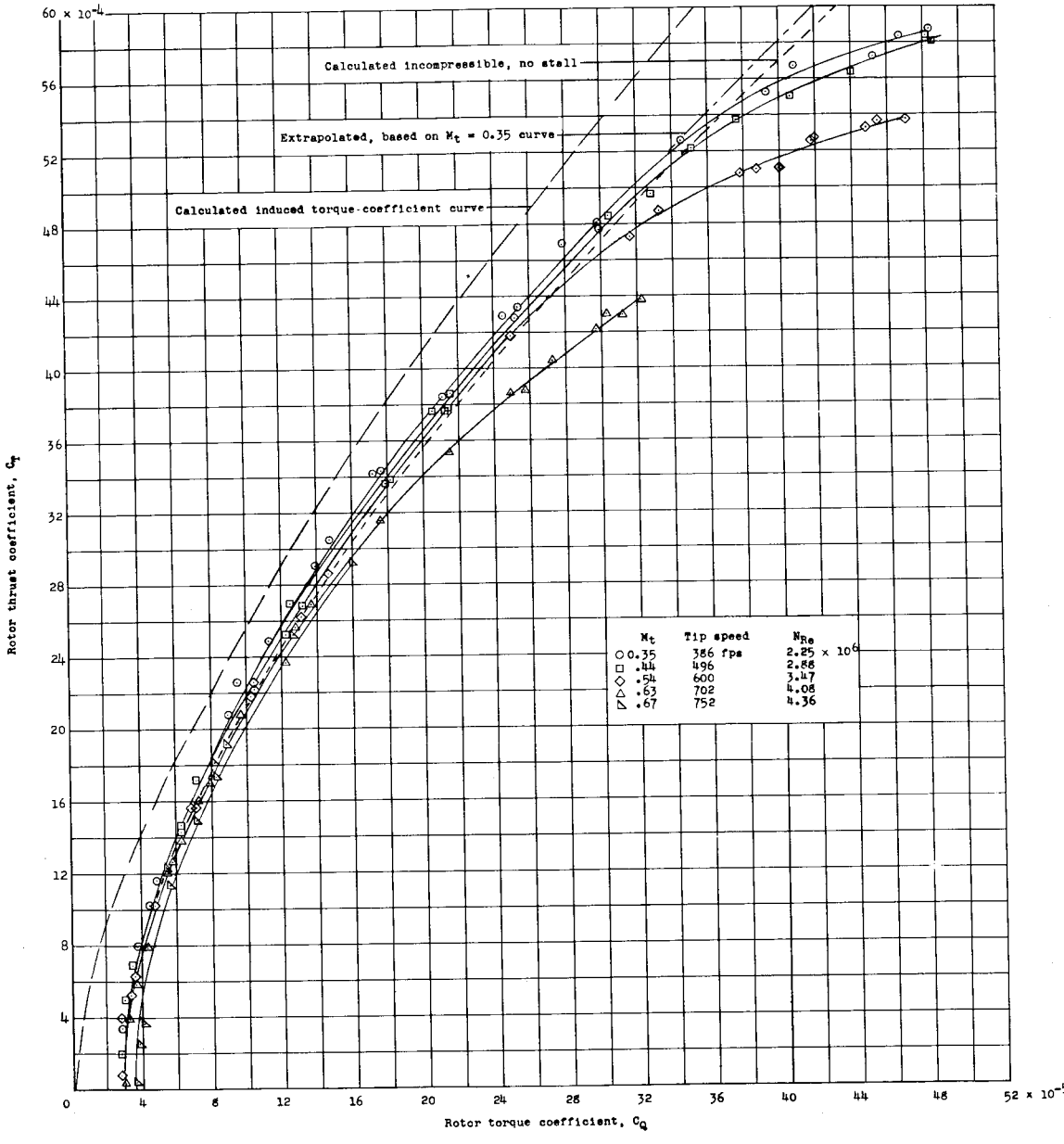

Figure 4.- Hovering performance of rotor blades having NACA 63_2A015 airfoil sections with a 230 mean line. Calculated incompressible curve based on $c_{d,o} = 0.0079 - 0.0216\alpha_r + 0.400\alpha_r^2$ and $c_l = 5.73\alpha_r$. $\sigma = 0.030$.

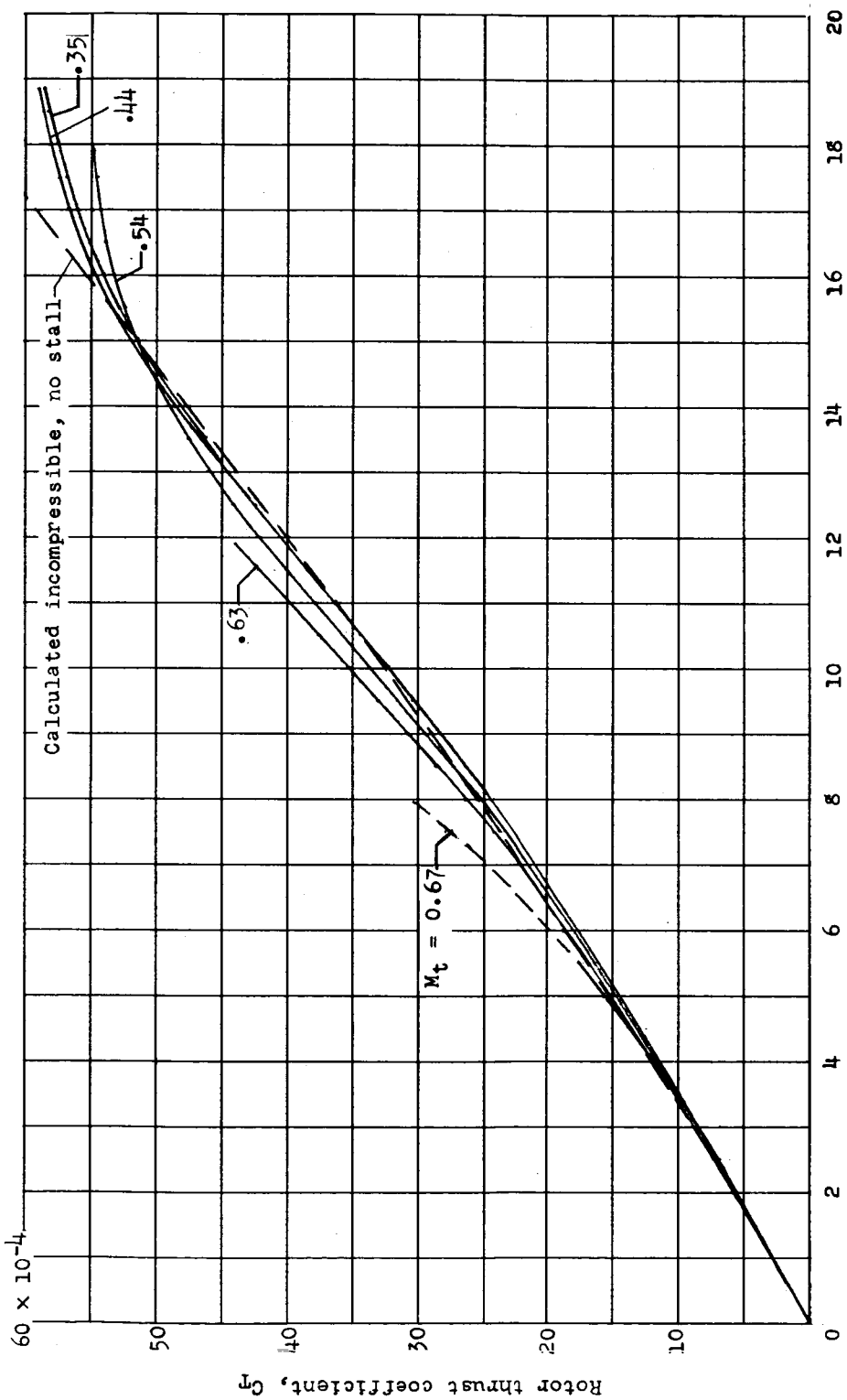

Figure 5.- Effect of tip Mach number on rotor thrust coefficient.

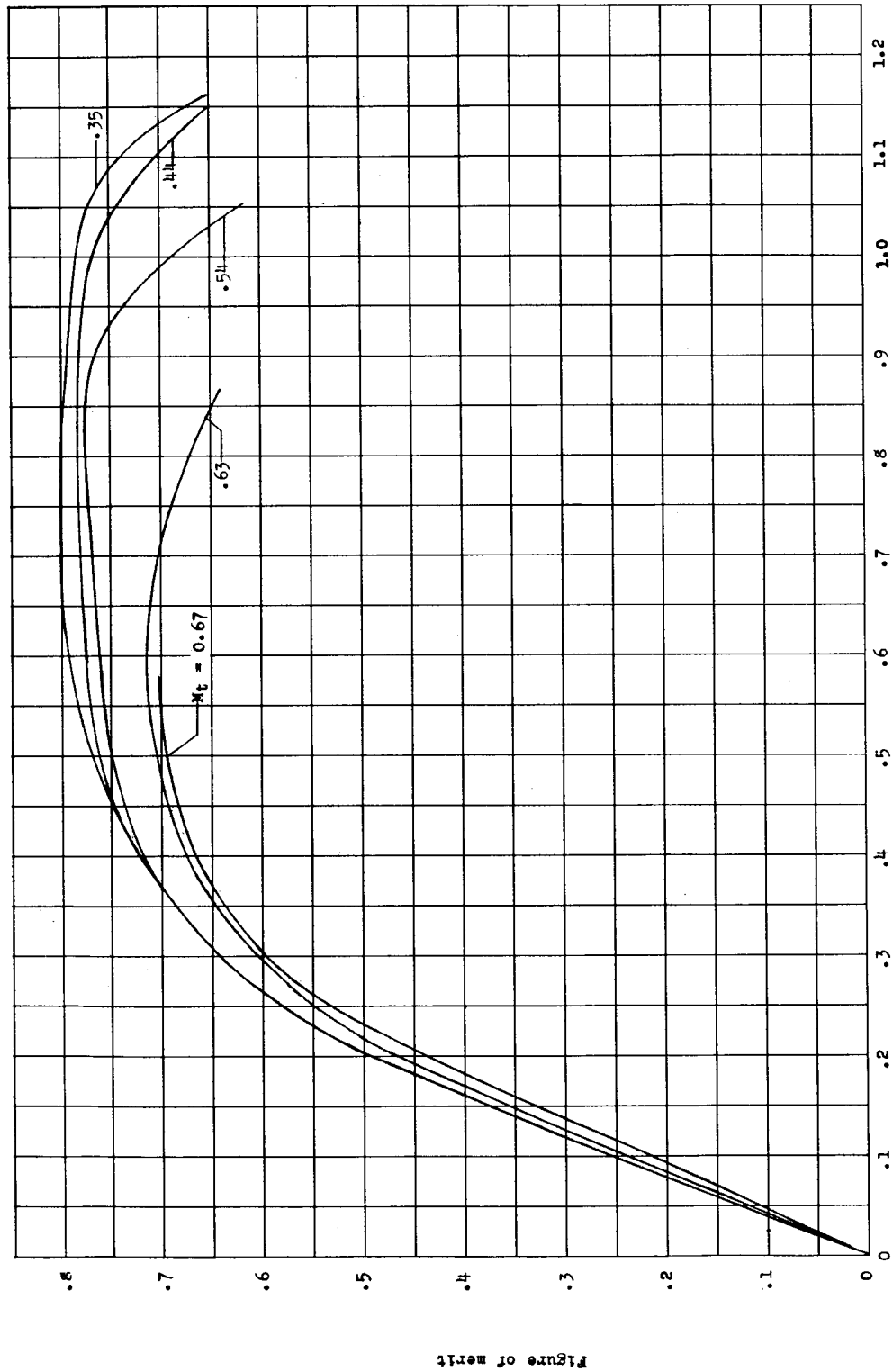

Figure 6.- Effect of tip Mach number on rotor figure of merit.

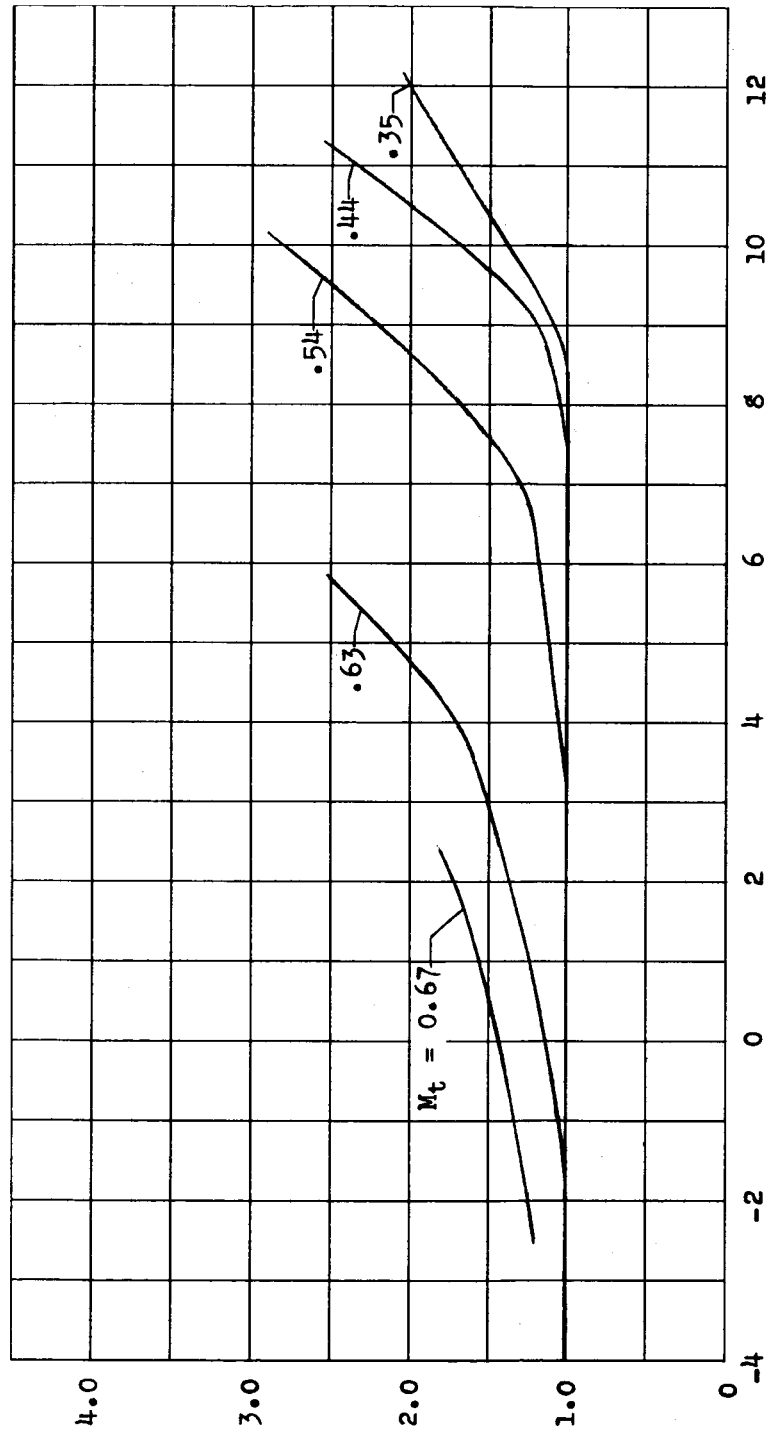

Figure 7.- Effect of tip angle of attack and Mach number on ratio of profile-drag torque coefficients. $\alpha_{r,t}$ corrected for dynamic twist.

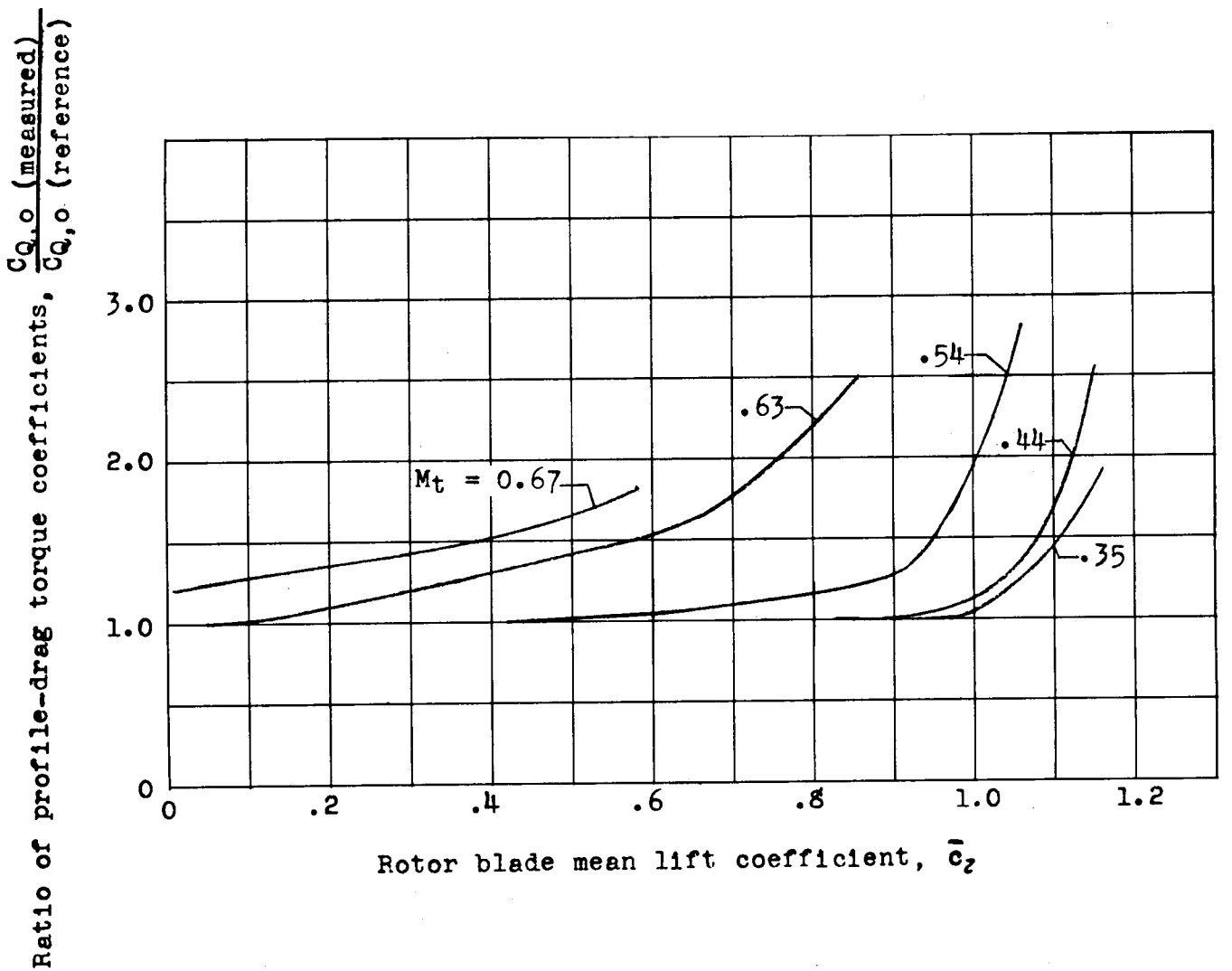

Figure 8.- Effect of rotor blade mean lift coefficient and Mach number on ratio of profile-drag torque coefficients.

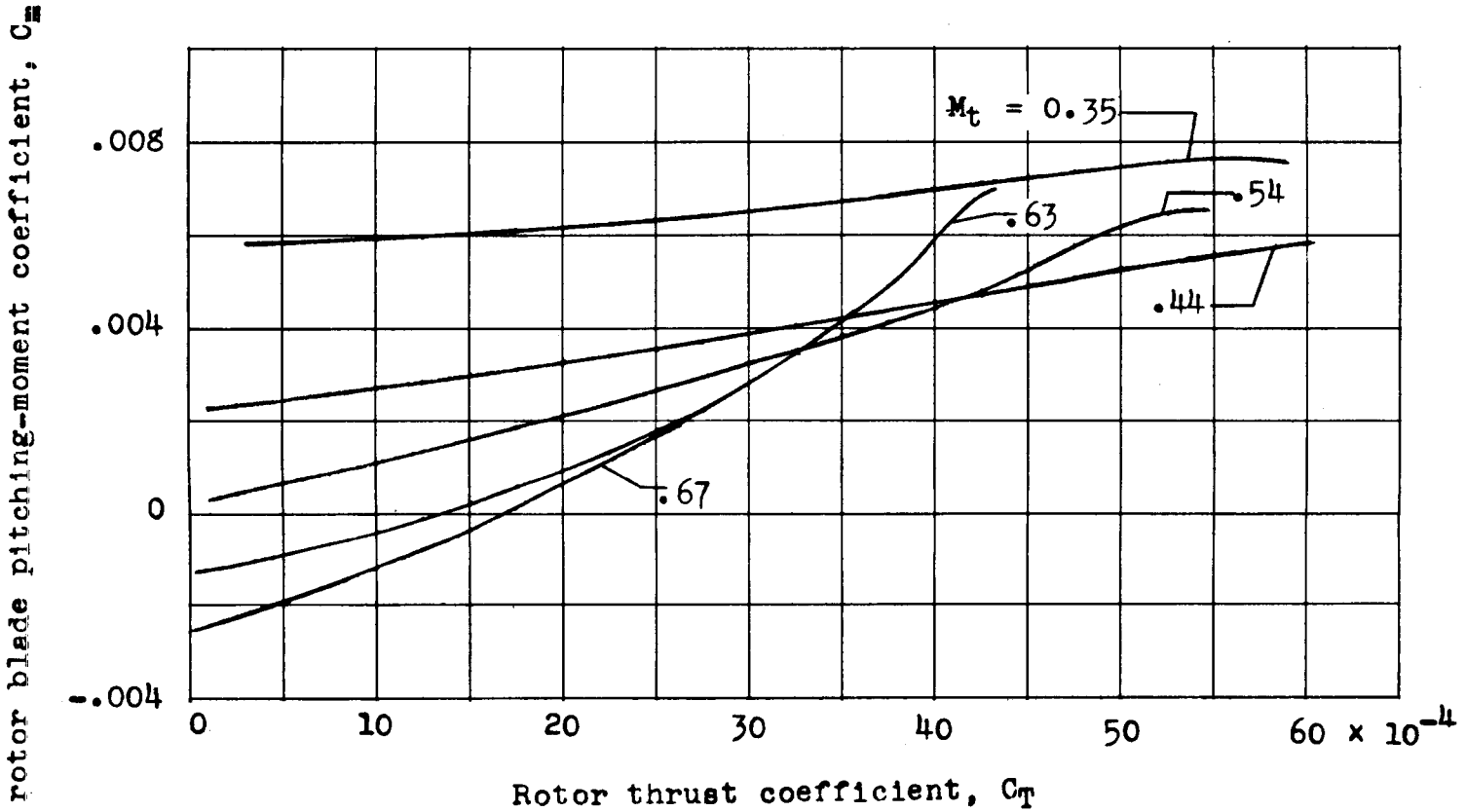

Figure 9.- Effect of tip Mach number on the rotor blade pitching-moment coefficients.

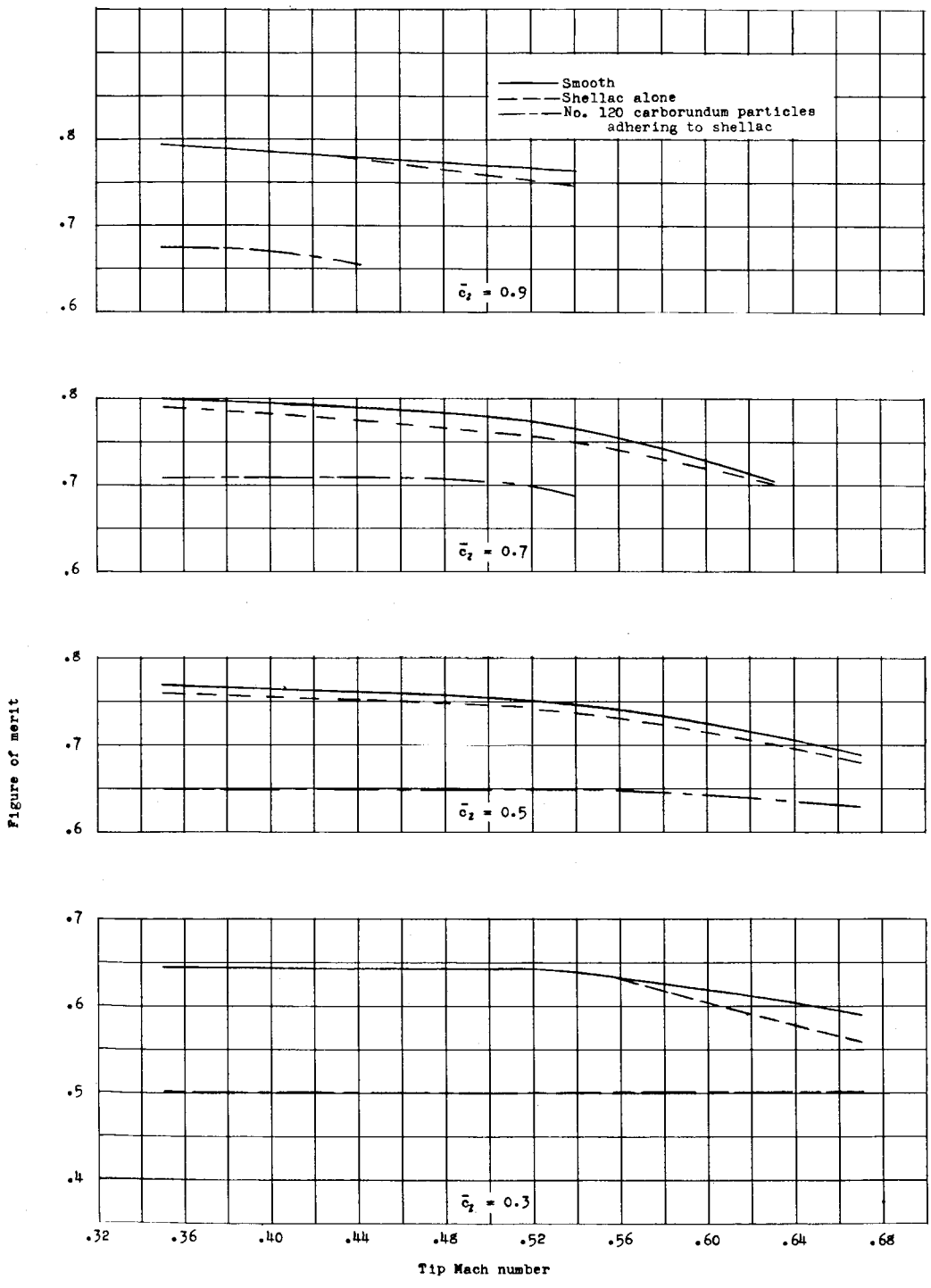

Figure 10.- Effect of leading-edge roughness and tip Mach number on rotor efficiency.

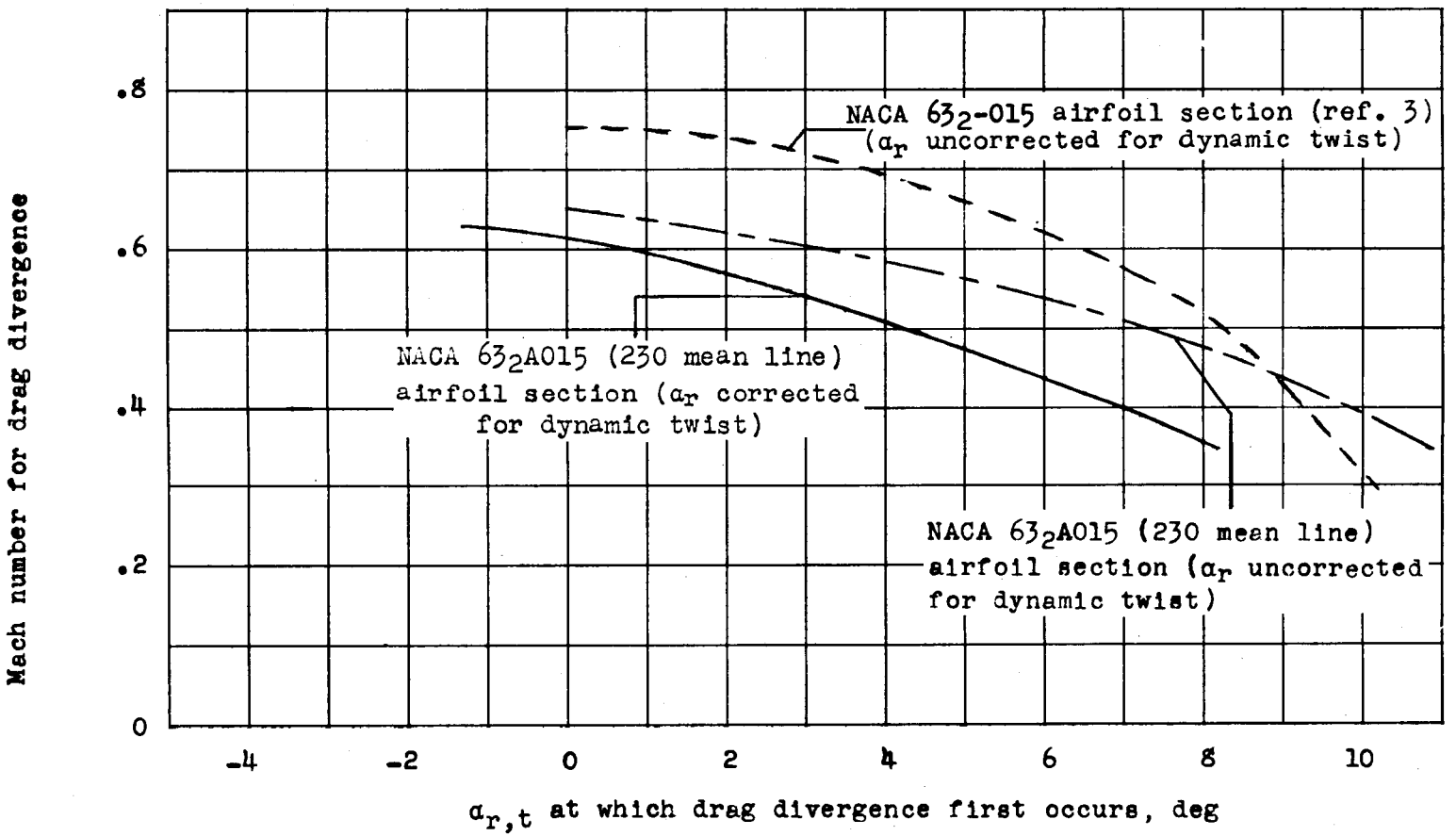

Figure 11.- Effect of Mach number and tip angle of attack on Mach number for drag divergence.

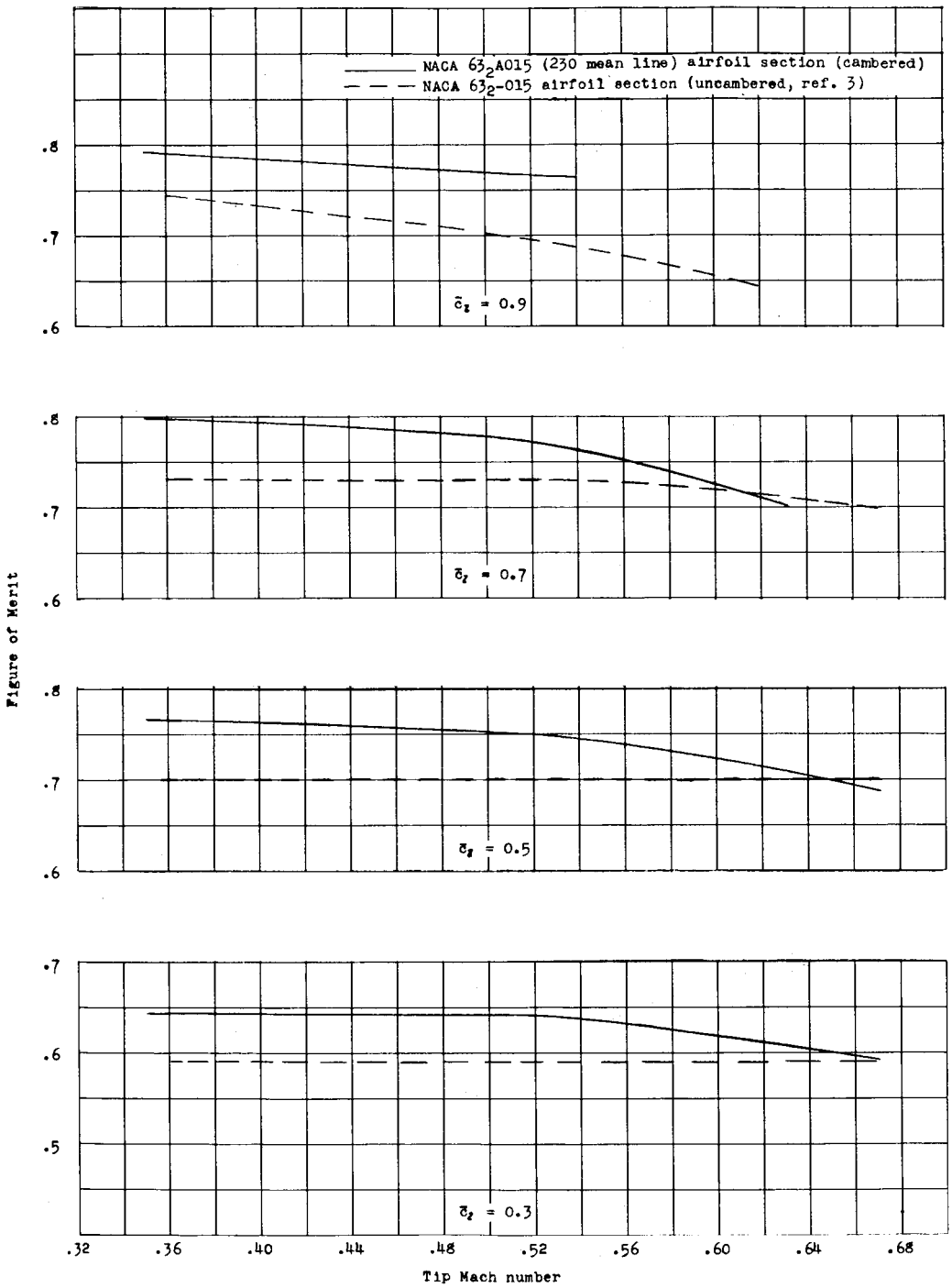

Figure 12.- Comparison of the effects of tip Mach number on rotor efficiency of cambered and uncambered rotor blades.